

# SAR Processing By Chirp Scaling Algorithm(CSA) Based General Algorithm

Dong-Hyun Kim (1), Do Chul Yang(1), Ho Ryung Jung(1), Dong Han Lee(1)

<sup>1</sup> Korea Aerospace Research Institute, 169-84 Gwahak-ro, Yuseong-gu, Daejeon, 34133, Korea  
Email: [kiyaes@kari.re.kr](mailto:kiyaes@kari.re.kr)

**KEY WORDS:** CSA, SAR focusing, TOPS, Sliding Spotlight, BAS

**ABSTRACT:** A SAR processing software needs to be properly designed for several available operational modes in the SAR mission. There are several algorithms that suit to specific operational modes. However, many algorithms in a SAR processing software can cost much on development and maintenance. So here, one CSA based general algorithm for many SAR missions is to be proposed, which incorporates a parameter  $\xi$  that helps effectively manipulate azimuth signal data. Optimizations of the parameter according to the different operational modes will be addressed and the processed results will be shown.

## 1. SAR operational characteristics

There are many SAR satellites under operation and will be. Each of them can have several operational modes like mono static or bi static and stripmap, scanSAR, TOPS, sliding spotlight, staring spotlight and so on. These modes have different levels of trade-off between scene length and resolution.

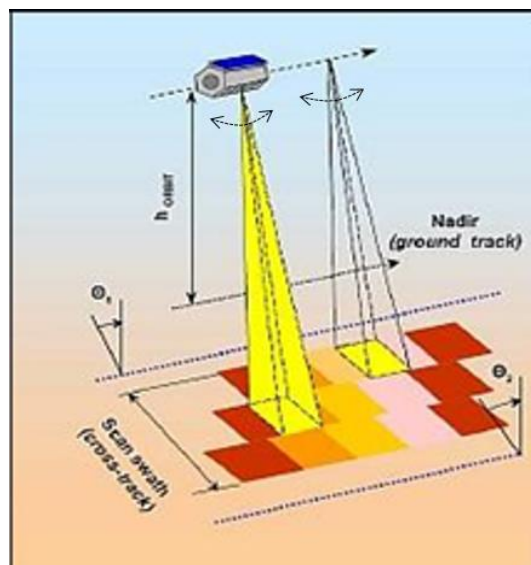


Figure 1. SAR mode operations

Figure 1 shows TOPS mode operation. Never the less, it could be thought as general operational mode except the specific azimuth beam steering of TOPS. Different subswaths are involved with different beam hardware parameter settings. So, general SAR operational mode can have any azimuth beam steering scheme with multiple beams of different hardware parameters.

It is preferred to have one general SAR raw data processing algorithm that can handle any operational mode data. It can provide high quality SAR products with low cost even in the case of arbitrary multiple beams combined operation with not good condition of hardware beams' parameters for processing or some raw data acquired by not typical operational modes but in between some typical modes, for instance, sliding spotlight but not exactly, and also close to staring spotlight operation.

So, the expected one general SAR processing algorithm should be able to process arbitrary azimuth bandwidth data, properly handle azimuth signal of the raw data and control the pixel resolution according to the azimuth beam steering scheme with multiple beams of hardware parameters.

## 2. Chirp Scaling Algorithm based General SAR Processing Algorithm

### 2.1 Algorithm flow

The proposing algorithm is based on Chirp Scaling algorithm incorporating two azimuth deramping processes. Range processing is the same as that of CSA, and in this paper, detailed description about it is omitted, and can be found in the well known text book. The figure below shows the flow diagram of the proposing one general algorithm.

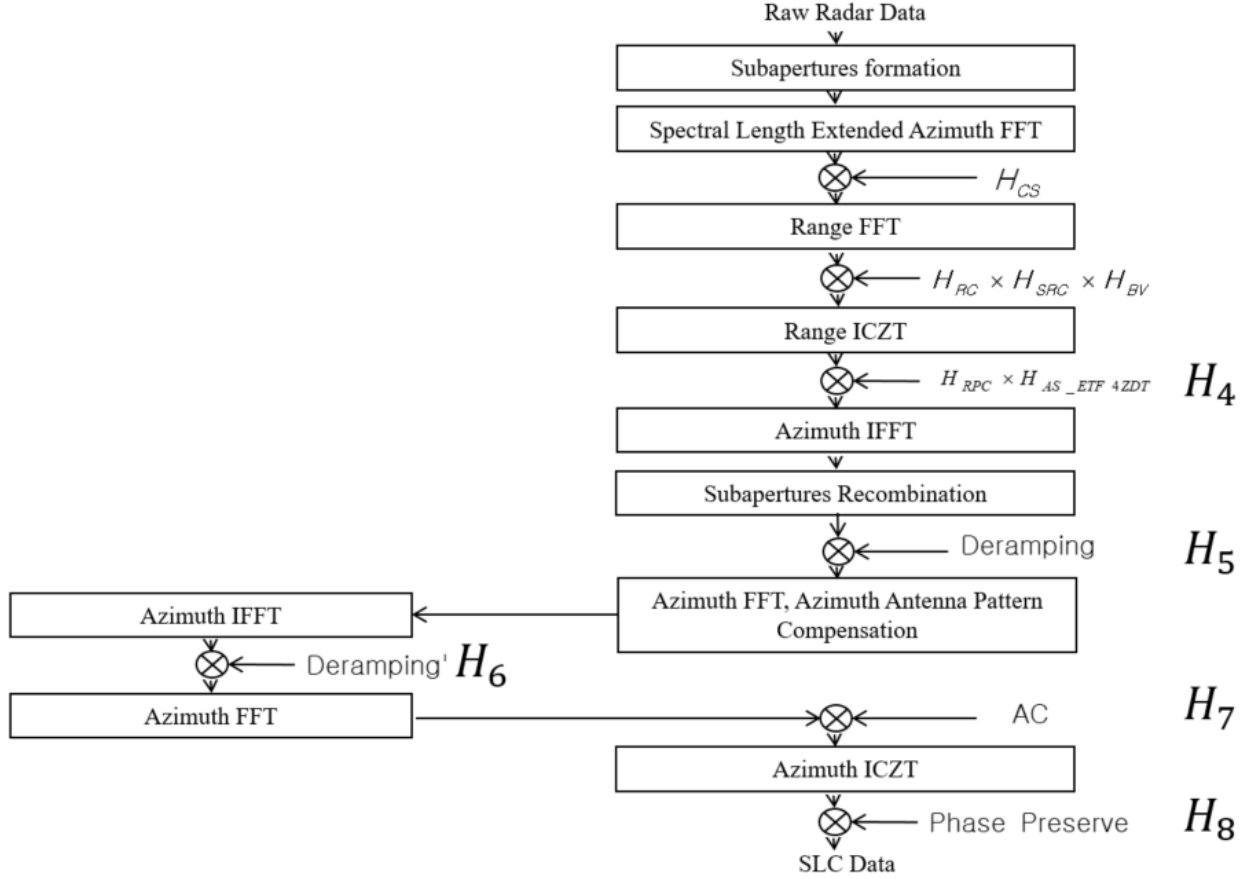


Figure 2. Flow diagram of Chirp Scaling algorithm based General SAR Processing Algorithm

The range processing flow of the proposed algorithm, until  $H_{RPC}$  at marked as  $H_4$  in the figure, which is that of the CSA, is the same as that described in the reference (Ian G. Cumming, Frank H. Wong, 2005).

The proposing algorithm starts by subaperture separation of the raw data and apply spectral length extension azimuth FFT for the subaperture data, not as usual short azimuth FFT. So, the number of subapertures can be freely selected for minimal integer as 1 or 2 or 3 or larger value suitable for the kinds of operational modes and the Nyquist criteria is always satisfied among the azimuth signal handling throughout the algorithm. Inverse chirp-z transformation is utilized for the range focusing and also for the azimuth focusing, not as usual IFFT. So, the image pixel spacings in azimuth and range domain can be freely controlled along the subswath of some specific beam. This helps the algorithm to achieve unified azimuth and range pixel spacings over multiple beams observed raw data and proper pixel spacings compared to the azimuth and range bandwidths of multiple beams data.

Proposing algorithm mainly adopts azimuth signal processing filters from  $H_4$  until  $H_8$ . Detailed mathematical formulas for them are as below.

$$H_4(f_a, r) = H_{AS\_ETF4ZDT} = M_1(w_\eta) \cdot \exp \left[ -j \frac{\pi}{K_{scl}(r)} f_a^2 \right] \quad (1)$$

$$\text{here, } K_{scl}(r) = -\frac{2v_{eff}^2(r)}{\lambda r_{scl}(r)}, \quad r_{scl}(r) = r \quad (2)$$

$$M_1(w_\eta) = \exp \left[ j \left\{ 2 \left( \frac{2\pi}{\lambda} + \frac{w_r}{c} \right) R_{r2}(\eta^*) + w_\eta \eta^* \right\} \right]$$

$$R_{r2}(\eta) = c_4 \eta^4 + (c_3 + 4c_4 t_1) \eta^3 + (c_2 + 3c_3 t_1 + 6c_4 t_1^2) \eta^2$$

$\lambda$  is the wavelength in meter of the carrier signal,  $r$  is the closest approach in meter between target and the antenna.  $f_a$  is the azimuth frequency in Hz,  $v_{eff}$  is effective velocity in m/sec,  $K_{scl}(r)$  is scaling Doppler rate in Hz/sec.

$M_1(w_\eta)$  is referred to the reference, (Jae Chul Yoon).

$$H_5(t_a, r) = \exp[-j\pi K_{rot\_geometry} \cdot (t_a - t_{mid})^2] \quad (3)$$

here,  $K_{rot\_geometry}(r) = K_{rot1}(r) = -\frac{2v_{eff}^2(r)}{\lambda r_{rot\_geometry}}$  and  $r_{rot\_geometry}$  is the geometrical beam rotation distance which can be referred to the reference (Pau Prats, Member, IEEE, Rolf Scheiber, Josef Mittermayer, Member, IEEE, Adriano Meta, Member, IEEE, and Alberto Moreira, Fellow, IEEE, Febr. 2010).

$$H_6(t_a, r) = \exp[-j\pi(K_{rot2}(r) - K_{rot\_geometry}) \cdot (t_a - t_{mid})^2] \quad (4)$$

here,  $K_{rot2}(r) = -\frac{2v_{eff}^2(r)}{\lambda r_{rot2}(r)}$  is the azimuth deramping Doppler rate and

$$r_{rot2}(r) = r \cdot \xi. \quad (5)$$

$\xi$  is the parameter to be set in accordance of the azimuth beam steering scheme with the beam hardware parameters. Azimuth compression is applied by the filter just below.

$$H_7(f_a, r) = \exp\left[j\frac{\pi}{K_{eff}(r)} f_a^2\right] \quad (6)$$

Here,  $K_{eff}(r) = K_{scl}(r) - K_{rot2}(r)$ . Finally the residual phase information is removed from the processed data by the filter as below.

$$H_8(t_a, r) = \exp\left[j\pi K_t(r) \cdot \left(1 - \frac{1}{\xi}\right)^2 \cdot (t_a - t_{mid})^2\right] \quad (7)$$

Here,  $K_t(r) = -\frac{2v_{eff}^2(r)}{\lambda \cdot r \cdot (\xi - 1)}$ . The general SAR processing algorithm with proper setting of the value of  $\xi$  will generate highly accurate SAR image datasets from arbitrary operational modes including stripmap, scanSAR, TOPS, sliding spotlight, staring spotlight and any in between.

## 2.2 $\xi$ setting

In order to handle the azimuth signal for proper processing, it is required that the azimuth bandwidth of any target is larger than 0 Hz after deramping by  $H_6$  and the azimuth time span of the processed scene is not extended too long compared to the azimuth time domain of the original raw data. Optimal setting of the value of  $\xi$  to satisfy the conditions mentioned above is described below.

In the case of operational mode is stripmap or scanSAR or TOPS, then

$$\xi = \frac{r_{rot\_geometry}}{r_{mid}}. \quad (8)$$

Here,  $r_{mid}$  is  $r$  of scene center. And in here, the calculated value of  $r_{rot\_geometry}$  is to be found again in a different way for stripmap or scanSAR mode as explained below.

If its calculation as definition causes numerical error then  $r_{rot\_geometry} = 1000 \cdot r_{mid}$ , if  $|r_{rot\_geometry}| > 1000 \cdot r_{mid}$  and  $r_{rot\_geometry} > 0$  then  $r_{rot\_geometry} = 1000 \cdot r_{mid}$ , if  $|r_{rot\_geometry}| > 1000 \cdot r_{mid}$  and  $r_{rot\_geometry} < 0$  then  $r_{rot\_geometry} = -1000 \cdot r_{mid}$ , if  $|r_{rot\_geometry}| \leq 1000 \cdot r_{mid}$  then  $r_{rot\_geometry}$  is set as calculated.

In the case of operational mode is sliding spotlight or staring spotlight or any in between them, then  $\xi$  is set depending on the two conditions as below. The first condition is about the processed scene length extension constrain.

$$\xi = 1 + \frac{\Delta t_{a0}}{\gamma_1 T_a - \Delta t_{a0}}, \gamma_1 > 0 \quad (9)$$

$T_a$  is the total azimuth time length of the raw data,  $\Delta t_{a0}$  is the processed azimuth scene length in seconds. Here, the range  $\frac{\Delta t_{a0}}{T_a} < \gamma_1 < 1.25$  can be used then, allowed  $\xi$  range is found.

$$\xi_{\min\_Y_1} = -\infty < \xi < 1 + \frac{\Delta t_{a0}}{1.25 \cdot T_a - \Delta t_{a0}} = \xi_{\max\_Y_1} \quad (10)$$

The second condition is about the target azimuth signal bandwidth constrain.

$$\xi = \frac{v_{eff}(r_{mid}) \cdot T_{obs}}{v_{eff}(r_{mid}) \cdot T_{obs} - \gamma_2 \cdot \theta_{az} \cdot r_{mid}}, \gamma_2 > 0 \quad (11)$$

$T_{obs}$  is a target observation duration in seconds,  $\theta_{az}$  is the 3dB azimuth beam width in radians. Here, the range  $1 < \gamma_2 < 0.75 \cdot \frac{B_{a\_Target}}{B_{FOV}}$  can be used then, allowed another  $\xi$  range is found.

$$\xi_{\min\_Y_2} = \frac{v_{eff}(r_{mid}) \cdot T_{obs}}{v_{eff}(r_{mid}) \cdot T_{obs} - \theta_{az} \cdot r_{mid}} < \xi < \frac{1}{1-0.75} = \xi_{\max\_Y_2} \quad (12)$$

Where,  $B_{a\_Target} = \frac{2v_{eff}^2(r_{mid})}{\lambda r_{mid}} \cdot T_{obs}$ ,  $B_{FOV} = \frac{2v_{eff}^2(r_{mid})}{\lambda r_{mid}} \cdot \frac{\theta_{az} \cdot r_{mid}}{v_{eff}(r_{mid})}$ .

The constant values above, 1.25 and 0.75 can be adjusted for tuning the processing.

Optimal value of  $\xi$  from the two conditions can be set as follow.

Here, let  $\Delta \xi_{one\ third\_Y_2} = \frac{\xi_{\max\_Y_2} - \xi_{\min\_Y_2}}{3}$ . In the case of  $\xi_{\max\_Y_2} \leq \xi_{\max\_Y_1}$  then,  $\xi = \frac{\xi_{\min\_Y_2} + \xi_{\max\_Y_2}}{2}$ . In the case of  $\xi_{\max\_Y_2} > \xi_{\max\_Y_1}$  and  $\xi_{\min\_Y_2} + \Delta \xi_{one\ third\_Y_2} \leq \xi_{\max\_Y_1}$  then,  $\xi = \frac{\xi_{\min\_Y_2} + \Delta \xi_{one\ third\_Y_2} + \xi_{\max\_Y_1}}{2}$ . In the case of  $\xi_{\max\_Y_2} > \xi_{\max\_Y_1}$  and  $\xi_{\min\_Y_2} + \Delta \xi_{one\ third\_Y_2} > \xi_{\max\_Y_1}$  then,  $\xi = \xi_{\min\_Y_2} + \Delta \xi_{one\ third\_Y_2}$ .

### 3. Test Result and Conclusion

Tests have been performed with KOMPSAT-5 raw data. Two operational modes datasets were used which are ST as of the stripmap mode and UH as of the sliding spotlight mode which is a bit close to spotlight mode. Processed image and azimuth processing accuracy measurements with  $\xi$  value used are shown below.



Figure 3. Processed image of UH mode

The image above is the proposing algorithm test result for the KOMPSAT-5 UH mode. There is a very small bright dot

like area in the left upper part of the image, which is the field where a corner reflector is located. This point target image is examined as below for measuring of the image quality.

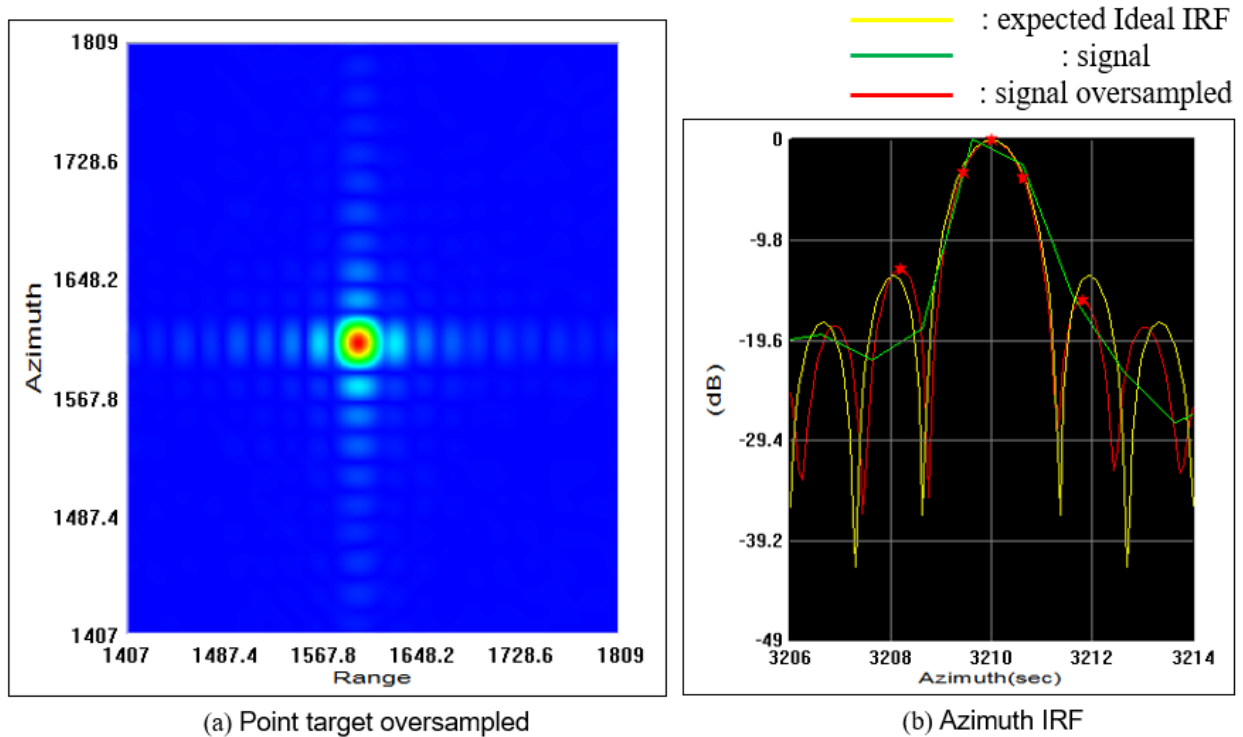


Figure 4. Point target oversampled contour plot and its azimuth impulse response function in the processed image of UH mode

Table 1. Proposing algorithm test result with KOMPSAT-5 raw data

Quality Measure \ Mode	ST	UH
	$\xi$	-1000
Azimuth Resolution (Meter)	2.102	0.559
Azimuth PSLR(dB)	-13.309	-12.557
Azimuth ISLR(dB)	-10.118	-10.527

As shown above in the case of K-5 UH mode, azimuth processing accuracy is a little bit degraded as the sidelobes of the azimuth IRF are unbalanced as shown in Figure 4 (b) and so the azimuth PSLR as shown on Table 1. This defect can be caused by inaccuracies in azimuth focusing parameter or in azimuth antenna pattern compensation. Otherwise, the proposed algorithm can be used for multi SAR system.

#### 4. References

Dong Hyun Kim. Method and system for inverse Chirp-z transformation. Republic of Korean Patent Application No. 10-1687658.

Ian G. Cumming, Frank H. Wong, 2005. Digital Processing of Synthetic Aperture Radar Data. Artech House Inc., pp. 283-322.

Jae Chul Yoon. Method for SAR Processing. European Patent Application No. 14 160 447.0.

Pau Prats, Member, IEEE, Rolf Scheiber, Josef Mittermaier, Member, IEEE, Adriano Meta, Member, IEEE, and

Alberto Moreira, Fellow, IEEE, Febru. 2010. Processing of Sliding Spotlight and TOPS SAR Data Using Baseband Azimuth Scaling. IEEE Trans. Geosci. Remote Sens., vol. 48, no. 2, pp. 770-780.